Contents list available at CBIORE journal website

International Journal of Renewable Energy Development

Journal homepage: https://ijred.cbiore.id

Research Article

Mathematical model to evaluate the effect of key operating conditions on proton exchange membrane fuel cell performance

Tan-Thich Do*, Trung-Kien Vi, Cong-Son Pham

Department of Electrical and Mechatronics, Lac Hong University, Vietnam

Abstract. Nowadays, proton exchange membrane fuel cells (PEMFCs) are regarded as a promising energy source for future applications due to their relatively low operating temperature, high efficiency, high power density, fast start-up capability, and zero emissions. During PEMFC operation, performance is influenced by numerous factors, including the key operating conditions. Therefore, developing a mathematical model to evaluate the effects of key operating conditions on PEMFC performance and energy efficiency is both necessary and significant in the PEMFCs. In this study, a mathematical model was developed using MATLAB/Simulink software and subsequently validated through a series of experiments to assess its accuracy. The results demonstrate that PEMFC performance is strongly affected by operating conditions, including operating temperature, operating pressure, membrane thickness, cathode gas type, cell active area, and the number of cells in the stack. In addition, water, heat generation, energy efficiency, and gas consumption were also considered and discussed detailed in the model. The findings indicate that operating temperature and pressure are the most influential parameters affecting PEMFC performance and energy efficiency. When the operating temperature increased, the cell performance improved due to enhanced electrochemical reaction kinetics and improved electrical conductivity. However, when the PEMFC operates at temperatures above 70 °C, a deterioration in performance is observed. This behavior can be attributed to membrane dehydration at elevated temperatures, which reduces proton conductivity and, consequently, lowers the output cell voltage. Increasing pressure reduces membrane resistance and interface contact resistance, leading to a decrease in voltage losses and an improvement in cell voltage. Therefore, the optimal operating tempearature was achieved at 70 °C in this study. At a current density of 0.5 A cm^{-2}, the cell voltages are 0.550, 0.559, 0.564, 0.568, 0.571, and 0.574 V for anode operating pressures of 1.0, 1.5, 2.0, 2.5, 3.0, and 3.5 atm, respectively. Overall, this study provides a reliable and precise tool for predicting PEMFC performance under varying operating conditions.

Keywords: Proton exchange membrane fuel cell; Fuel cell voltage; Fuel cell power; Energy efficiency; Water generation; Heat generation; Hydrogen utilization; Oxygen utilization.

Received: 30th Dec 2025; Revised: 28th May 2026 ; Accepted: 30th June 2026; Available online: 11th July 2026

1. Introduction

Nowadays, proton exchange membrane fuel cells (PEMFCs) are considered one of the most promising energy sources for future applications due to their outstanding characteristics, such as high energy density, high power density, high efficiency, relatively low operating temperature, fast start-up capability, and zero emissions (Barbir, 2012). PEMFCs have been widely applied in portable power systems, stationary power systems, unmanned aerial vehicles (UAVs), and unmanned underwater vehicles (UUVs) (Boas *et al.*, 2022; Carrette *et al.*, 2001; Dyer, 2002).

The performance of proton exchange membrane fuel cells (PEMFCs) is influenced by numerous factors, including operating conditions and structural design. (Li *et al.*, 2025) studied the dynamic performance of the PEMFC under varying operating conditions based on the electrical-thermal-water integrated model. They indicated that the equipment operating states, time scales, and operating conditions influenced the operating efficiency and characteristics of internal safety of the PEMFC. (Rohendi *et al.*, 2015) investigated the effects of operating temperature and pressure on PEMFC performance degradation. Their results showed that membrane drying and cracking occurred at 80 °C after 100 h of operation, leading to significant performance degradation. (Zhao *et al.*, 2025) investigated the temperature distribution of the PEMFC under various operating conditions. Their results showed that the distribution of the temperature was non-uniform when the fuel cell load level increased. Hot spots occurred near the anode and cathode inlets and outlets and expanded to the center region of the fuel cell. (Murthy *et al.*, 2002) examined the effects of operating temperature and pressure on PEMFC performance while considering CO concentration and catalyst poisoning. They reported that the poisoning rate was reduced by a factor of four during their experiments. (Belkhiri *et al.*, 2011) evaluated PEMFC voltage under varying operating temperatures and membrane water contents, demonstrating that both parameters significantly affect cell performance. (Arat & Çeper, 2025) investigated the instantaneous temperature variations on the PEMFC performance under cold climate conditions. They revealed that when the PEMFC operated at −13, −14, and −15 °C, the cell voltage was reduced by 19%. (Giner-Sanz *et al.*,

* Corresponding author
Email: dotanthich@lhu.edu.vn (T-T Do)

https://doi.org/10.61435/ijred.2026.62184
ISSN: 2252-4940/© 2026.The Author(s). Published by CBIORE

2015) developed a statistical model to analyze PEMFC voltage under different operating conditions and concluded that the model showed good agreement with experimental results. (Santarelli & Torchio, 2007) conducted a series of experiments to investigate the influence of variable operating conditions on PEMFC voltage, providing valuable insights into their significant impact on cell performance. (Mohtadi *et al.*, 2005) studied the effect of operating temperature on hydrogen sulfide adsorption at the anode and found that sulfur species are more strongly adsorbed at lower temperatures. (Zhao *et al.*, 2015) analyzed local temperature distribution and parameter sensitivity in a PEMFC system, showing that temperature not only affects the output voltage but also has a significant impact on membrane water content. (Mus *et al.*, 2025) experimented to evaluate the effect of the ambient on the PEMFC performance. They revealed that the best performance was achieved at 35 °C and relative humidity of 75%. (Chugh *et al.*, 2020) combined modeling and experiments to evaluate the effects of operating temperature, pressure, and humidity on PEMFC performance, achieving model prediction errors in the range of 7–15%. (Kim & Hong, 2008) investigated the effects of humidity and temperature on PEMFC voltage and revealed that cell performance is strongly influenced by operating temperature and humidity. (Park & Li, 2006) developed a mathematical model to analyze the effects of temperature and flow distribution on PEMFC output voltage. Their results indicated that, under sufficiently uniform reactant flow conditions, temperature becomes the dominant factor affecting voltage variation when flow non-uniformity is minimal. (Atak *et al.*, 2023) examined the effects of operating pressure and temperature on PEMFC performance by analyzing key thermodynamic parameters, including entropy generation, exergy destruction, exergy efficiency, and thermal efficiency. At a current density of 1 A cm^{-2}, the exergy efficiency increased by 13.17% as the operating temperature rose from 303 to 363 K. (Lu *et al.*, 2019) developed a PEMFC model using ANSYS FLUENT, which showed good agreement with experimental data. (Wang *et al.*, 2025) optimized the distribution of the temperature in a PEMFC under six configurations of cooling plates using the computational method. They indicated that the serpentine design achieved the lowest variation of the pressure, resulting in the best configuration, while (González *et al.*, 2025) studied the distribution of the temperature and current density on the PEMFC performance under different flow field channels. Their results show that the tapered design configuration is the best performance owing to the uniform current density and temperature. (Ozen *et al.*, 2016) evaluated PEMFC performance under various operating temperatures and reactant gas humidities, concluding that higher operating temperatures and inlet gas humidities significantly enhance performance. (Laribi *et al.*, 2018) investigated the effects of air temperature ranging from 60 to 140 °C on PEMFC performance by measuring impedance and employing artificial neural networks (ANNs). They demonstrated that the proposed model can be used to diagnose PEMFC operating conditions, such as flooding and membrane drying. (Shan & Choe, 2006) developed a three-dimensional computational fluid dynamics (CFD) model to simulate the influence of operating temperature on PEMFC performance, focusing on its effects on cathode humidity and membrane water content. (Amirfazli *et al.*, 2018) studied the influence of manifold geometry on temperature distribution and found that reducing flow-field channel dimensions improves temperature uniformity. (Faddeev *et al.*, 2021) developed a CFD model to analyze the effects of ambient conditions on the performance of open-cathode PEMFCs. Their model showed good agreement with experimental results, with errors below 10%, and indicated that optimal performance was achieved at ambient temperatures below 20 °C. Finally, (Lee & Chu, 2007) investigated the effect of operating temperature on liquid–gas distribution within PEMFCs and reported that excessive water accumulation leads to channel blockage, deteriorating mass transport, and reducing overall performance.

(Ghasemi *et al.*, 2017) developed a three-dimensional (3D) model to investigate the effects of six different cooling flow-field designs on PEMFC performance, including conventional serpentine, conventional parallel, conventional spiral, parallel–serpentine, typical MPSFFs, and typical serpentine configurations. They concluded that the conventional spiral flow field provides superior performance. (Lee *et al.*, 2023) experimentally evaluated PEMFC performance degradation under various operating temperatures and humidity levels. Their results showed that performance degradation accelerated at a relative humidity of 10%, and the degradation rate increased from 25.2% to 75.71% as the temperature rose to 90 °C. (Tiss *et al.*, 2013) developed a model based on mass and energy conservation equations to analyze the effect of operating temperature on PEMFC voltage, demonstrating good agreement with real-time control data. (Hu *et al.*, 2021) investigated and optimized operating temperature effects on PEMFC performance for electric vehicle applications, reporting an efficiency improvement ranging from 15% to 28.7%. (Waller *et al.*, 2016) evaluated PEMFC performance under different operating temperatures, pressures, and hydrogen dilution levels, and found that these parameters significantly influence the output voltage. (Tang *et al.*, 2023) proposed a Takagi–Sugeno fuzzy model combined with model predictive control to analyze and regulate the influence of operating temperature on the output voltage of an 80 kW PEMFC system, achieving enhanced dynamic performance under varying operating conditions. (Chen *et al.*, 2019) investigated gas diffusion layer (GDL) characteristics, focusing on the influence of polytetrafluoroethylene (PTFE) content on PEMFC performance, and reported increased hydrophobicity with higher PTFE loading. In contrast, Flick et al. (Flick *et al.*, 2014) examined PEMFC material characteristics and demonstrated that voltage has a significant impact on overall performance. (Ding *et al.*, 2023) analyzed the effects of pinhole size on PEMFC performance and revealed that the capillary pressure associated with a 10 μm pinhole is lower than that of a 100 μm pinhole. (Xia *et al.*, 2021) optimized GDL properties by focusing on porosity and thickness, achieving a 7.7% performance improvement at optimal cathode and anode thicknesses of 140 – 170 μm and 40 – 120 μm, respectively, with an optimal porosity range of 35 – 45%. (Santarelli *et al.*, 2006) developed an analytical model to estimate PEMFC voltage over an operating temperature range of 50 – 80 °C and concluded that temperature significantly affects output voltage. (Hao *et al.*, 2023) investigated the effects of current density distribution, water content, humidity, inlet gas pressure, and temperature on PEMFC voltage, reporting optimal water content and humidity at 0.2 MPa and 100%, respectively. (Noorkami *et al.*, 2014) evaluated the cell voltage under the effect of the operating temperature uncertainty. They indicated that the operating temperature was the key parameter to evaluate the cell performance. To improve the performance of the PEMFC, the humidity and temperature should be managed. The PEMFC performance is enhanced with control and conducted by (Ou *et al.*, 2017). Their results show that the improvement of PEMFC increased up to 10%, while (Chen *et al.*, 2024) proposed a temperature control strategy to achieve high performance of the PEMFC using intelligent algorithms.

(Neyerlin *et al.*, 2005) studied the effect of humidity on the reduction of oxygen. They revealed that the cell voltage lost about 20 mV at a relative humidity of 30%. (Jomori *et al.*, 2012) studied the degradation of the fuel cell performance under the effect of the oxygen transport. They indicated that the performance decayed at high load levels owing to an increase in the transport overpotential. (Radhakrishnan & Haridoss, 2011) evaluated the PEMFC performance under the condition of GDL compression. Their results indicated that the GDL compression significantly affected the pressure drop on the parallel channel flow field and the serpentine channel flow field. (Chang *et al.*, 2007) investigated the effect of clamping pressure on the PEMFC performance. They revealed that when the clamping pressure increased, the ohmic resistance reduced, resulting in improved performance. Similarly, (Bates *et al.*, 2013) was also studied the effect of clamping pressure. (Larbi *et al.*, 2013) studied the porosity characteristics and pressure on the output voltage of the PEMFC. They indicated that the porosity increased, leading to the electrical conductivity decreased. (Zhou & Wu, 2007) developed a model to evaluate effect of the compression of GDL porosity on PEMFC performance. Their results show that the when the compression deformation increased, the output performance reduced.

In the last study (Diab *et al.*, 2025) developed the mathematical model of the PEMFC using the Newton–Raphson iterative method. Their model achieves high accuracy with a relative error of 0.5%. However, the influence of operating conditions on the PEMFC is not considered. Based on the aforementioned literature, PEMFC performance is influenced by numerous factors during operation. Although many studies have investigated these effects, comprehensive reports that simultaneously consider multiple operating and design parameters remain limited. Therefore, this study develops a mathematical model to evaluate the influence of operating conditions on PEMFC performance while accounting for various factors, including operating temperature, operating pressure, membrane thickness, water content, cell active area, cathode gas type, exchange current density, and the number of cells in a stack. In addition, gas consumption and energy efficiency of the PEMFC are analyzed in detail. First, the mathematical model is developed using MATLAB/Simulink. The model is then validated against experimental data to verify its accuracy. Finally, the effects of different operating conditions on PEMFC performance are systematically discussed and analyzed. This study provides a reliable and high-precision approach for predicting PEMFC performance under varying operating conditions.

2. Method

2.1 System description

Fig. 1(a) depicts the PEMFC operation in this study. The PEMFC converts the chemical energy into electrical energy directly. In addition, the products consisted of water and heat generation owing to the electrochemical reaction. The hydrogen gas and oxygen gas or air were supplied at the anode and cathode sides,

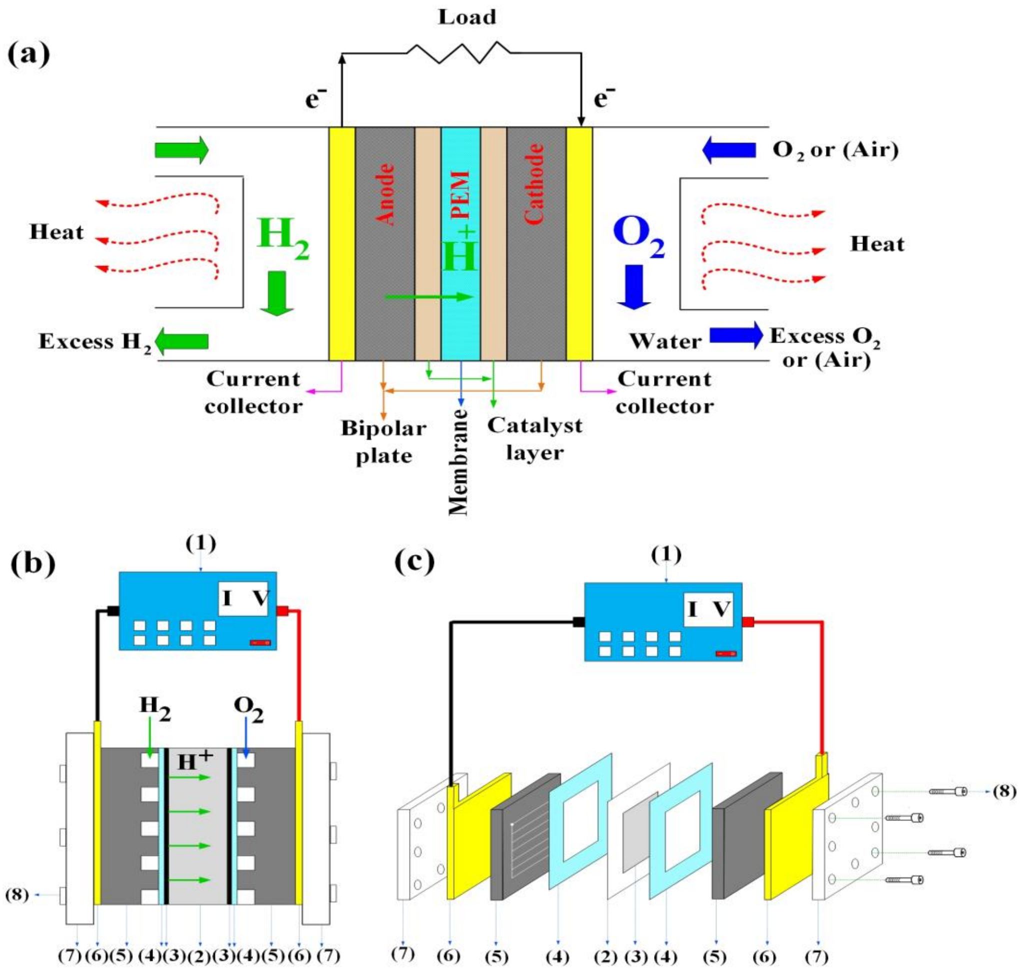

Fig. 1 Illustration of the PEMFC operation (a); Schematic of the PEMFC components (b); and exploded view of the PEMFC components (c)

Table 1
The function of the PEMFC components

Position	Component	Function
(1)	Electric load	It was used to apply the load to the PEMFC
(2)	Membrane	Here occurred the electrochemical reaction between the anode and cathode sides.
(3)	Catalyst layer	It was employed to enhance and catalyse the electrochemical reaction in PEMFC.
(4)	Gasket	It was used to prevent the gas leak.
(5)	Bipolar plate	The gas was conducted in the flow field channel. The hydrogen and oxygen were supplied at the anode and cathode side, respectively.
(6)	Current collector	It was used to conduct electricity.
(7)	End plate	It was assembled at the most outside of the anode and cathode sides.
(8)	Bolts and nuts	To keep the components tight in a fuel cell stack.

respectively. The electrochemical reaction occurred inside the membrane with the oxidation and reduction process, corresponding to the anode and cathode side, as follows the Eqs (1) and (2):

$$\mathrm{H_2} \rightarrow 2\mathrm{H^+} + 2\mathrm{e^-} \quad (1)$$

$$\frac{1}{2}O_2 + 2\mathrm{H^+} + 2\mathrm{e^-} \rightarrow H_2O \quad (2)$$

$$\mathrm{H_2} + \frac{1}{2}O_2 \rightarrow H_2O + Electricity + Heat \quad (3)$$

Fig. 1(b) and (c) present a schematic diagram and exploded view of the PEMFC components considered in this study. The PEMFC components consist of a membrane, catalyst layers, bipolar plates, current collectors, and end plates. In addition, the functions of the individual PEMFC components are summarized in Table 1.

2.2 Model development

In this study, the mathematical model of the PEMFC was developed in MATLAB/Simulink environment software. The description of the performance, water and heat generation, gas utilization, energy efficiency, and boundary conditions were presented in detail as follows.

2.2.1 Cell voltage in PEMFC

The cell voltage consists of a reversible voltage and irreversible voltage losses. The irreversible voltage accounts for various losses, including activation, ohmic, and concentration voltage losses. Accordingly, the cell voltage can be expressed as follows:

$$V_{\mathrm{cell}} = E_{\mathrm{Nernst}} - \eta_{\mathrm{act}} - \eta_{\mathrm{ohmic}} - \eta_{\mathrm{conc}} \quad (4)$$

Where: V_{cell} , E_{Nernst} , η_{act} , η_{ohmic} , and η_{conc} represent the cell voltage, reversible voltage, activation voltage loss, ohmic voltage loss, and concentration voltage loss, respectively. All these values are in units of V.

2.2.2 Reversible voltage

The reversible voltage represents the maximum theoretical cell voltage when the PEMFC operates under standard conditions (25 °C and 1 atm). Eq. (5) is used to calculate the reversible voltage of the PEMFC:

$$E_r = \frac{-\Delta G}{nF} = \frac{237340}{2.96485} = 1.229\ (V) \quad (5)$$

Where: ΔG represents the Gibbs free energy of the electrochemical reaction, in (J mol^{-1}); n denotes the number of electrons exchanged, $n = 2$; and F refers to Faraday's constant ($F = 96485\ J\ mol^{-1}$).

During the PEMFC operation in applications, the temperature and pressure were varied and were different from the standard conditions. Thus, the reversible voltage of PEMFC can be determined through the Nernst equation, which is represented by the relationship between operating temperature and pressure, as follows:

$$E_{Nernst} = E_r - \frac{\Delta S}{nF}(T - T_0) + \frac{RT}{nF}\ln\left(\frac{p_{H_2}p_{O_2}^{0.5}}{p_{H_2O}}\right) \quad (6)$$

Where: ΔS is the entropy change of the electrochemical reaction (J mol^{-1} K^{-1}); T denotes the operating temperature, in K; T_0 represents the reference temperature, in K; R is the ideal gas constant ($R = 8.314\ J\ mol^{-1}K^{-1}$); p_{H_2} refers to the partial pressure of the hydrogen (atm); p_{O_2} is the partial pressure of the oxygen (atm); and p_{H_2O} denotes the partial pressure of the water (atm).

The partial water vapor pressure depends on the operating temperature of the fuel cells. It was calculated by Eq. (7):

$$log(p_{H_2O}) = -2.1794 + 0.02953(T - 273.2) - 9.1837 \times 10^{-5}\,(T - 273.2)^2 + 1.4454 \times 10^{-7}(T - 273.2)^3 \quad (7)$$

The partial pressure of the hydrogen and the partial pressure of the oxygen, in atm, were determined corresponding to Eqs (8) and (9):

$$p_{H_2} = \frac{1}{2}\left[\frac{P_{H_2}}{e^{\frac{1.653i}{T^{1.334}}}}\right] - p_{H_2O} \quad (8)$$

$$p_{O_2} = \left[\frac{P_{air}}{e^{\frac{4.192i}{T^{1.334}}}}\right] - p_{H_2O} \quad (9)$$

Where: P_{H_2} and P_{air} denote the operating pressure at the anode side and cathode side, respectively.

2.2.3 Activation voltage loss

The activation voltage loss occurred when the PEMFC operated at low current density. The activation voltage loss represented the kinetics of the electrochemical reaction for both the anode side and the cathode side. It was calculated based on Tafel's equation by Eq. (10)

$$\eta_{\text{act}} = \eta_{\text{act,c}} + \eta_{\text{act,a}} = \frac{RT}{\alpha_c F}\ln\left(\frac{i}{i_{0,c}}\right) + \frac{RT}{\alpha_a F}\ln\left(\frac{i}{i_{0,a}}\right) \quad (10)$$

Where: $\eta_{\text{act,c}}$ denotes the activation voltage loss at the cathode side, in V; $\eta_{\text{act,a}}$ is the activation voltage loss at the anode side, in V; α_c denotes the coefficient of the charge transfer at the cathode side; α_a refers to the coefficient of the charge transfer at the anode side; i is the operating current density (A cm^{-2}); $i_{0,c}$ represents the exchanged current density at the cathode side (A cm^{-2}); and $i_{0,a}$ denotes the exchanged current density at the cathode side (A cm^{-2}).

2.2.4 Ohmic voltage loss

The ohmic voltage loss of the PEMFC represents the voltage loss due to resistance in the membrane, and resistance in the interconnector, such as bipolar plates, current collectors. Eq. (11) was employed to determine the ohmic voltage loss of the PEMFC.

$$\eta_{\text{ohmic}} = i(R_{\text{m}} + r_i) \quad (11)$$

Where: R_{m} and r_i denote the resistance in the membrane, in Ω; and the resistance in the interconnector, including the bipolar plates, current collectors, in Ω, respectively.

The resistance in the membrane depends on operating temperature and water content in the membrane. Eq. (12) can be used to calculate the ohmic voltage loss of the PEMFC:

$$R_m = \frac{t_m}{A_{fc}(0.00514\lambda - 0.00326)\, exp\left[1268\left(\frac{1}{T} - \frac{1}{303}\right)\right]} \quad (12)$$

Where t_m represents the thickness of the membrane, in cm; and A_{fc} denotes the activation area of the PEMFC, in cm^2.
The water content in the membrane depends on the water activity. It can be determined following Eq. (13).

$$\begin{cases} \lambda = 0.043 + 17.81a_m - 39.95a_m^2 + 36.0a_m^3 & 0 < a_m \le 1 \\ \lambda = 14.0 + 1.4\,(a_m - 1) & a_m > 1 \end{cases} \quad (13)$$

Where: a_m denotes the water activity. Generally, the water activity was selected as 0.5 (Zhu *et al.*, 2019), which was calculated as the average water activity at the anode and cathode sides.

2.2.5 Concentration voltage loss

The concentration voltage loss refers to the voltage drop caused by mass transport limitations when the reactant concentration, especially oxygen at the cathode, becomes insufficient at high current densities. It was determined by Eq. (14):

$$\eta_{\text{conc}} = \frac{RT}{nF} ln\left(\frac{i_L}{i_L - i}\right) \quad (14)$$

Where: i_L represents the limiting current density of the PEMFC, in A cm^{-2}.

The limiting current density of the PEMFC in this study was defined by Eq. (15):

$$i_L = nFh_m\left[\frac{C_{in} - C_{out}}{ln\left(\frac{C_{in}}{C_{out}}\right)}\right] \quad (15)$$

Where: h_m, C_{in}, and C_{out} refer to the mass transport coefficient at the cathode, in m s^{-1}; inlet oxygen concentration, in mol m^{-3}; and outlet oxygen concentration, in mol m^{-3}, respectively.

2.2.6 Stack voltage and power

In practice, the single cell was connected to multiple cells to increase the voltage and power. It was called a PEMFC stack. The stack voltage and stack power of the PEMFC were determined by Eq. (16) and Eq. (17), respectively.

$$V_{st} = N_{cell} \times V_{\text{cell}} \quad (16)$$

$$P_{st} = I_{cell} \times V_{\text{st}} \quad (17)$$

Where: V_{st} is the stack voltage, in V; N_{cell} denotes the number of cells in a stack; P_{st} represents the stack power, in W; and I_{cell} refers to the operating current of the PEMFC stack, in A.

2.2.7 Water and heat generation

During the PEMFC under load levels, the chemical energy from the fuel and oxidant is converted to generate electricity directly. In addition, the water and heat are produced owing to the electrochemical reaction. Thus, the water and heat generation of a PEMFC are considered in this study. Equations (18) and (19) expressed the amount of water and heat generation in PEMFC, respectively, as follows:

$$\dot{m}_{H_2O} = \frac{N_{cell} \times I_{cell}}{4F} M_{H_2O} \quad (18)$$

$$Q_{st} = N_{cell}(1.25 - V_{cell})I_{\text{cell}} \quad (19)$$

Where: M_{H_2O} denotes the molar mass of water, ($M_{H_2O} = 18\ g\ mol^{-1}$).

2.2.8 Gas utilization and energy efficiency of the PEMFC

During PEMFC operation, the hydrogen and oxygen (or air) were supplied to the anode and cathode side, respectively. At the anode side, the hydrogen consumption flow rate owing to the electrochemical reaction was determined by Eq. (20):

$$\dot{m}_{H_2} = \frac{N_{cell} \times I_{cell}}{2F} M_{H_2} \quad (20)$$

Where: M_{H_2} denotes the molar mass of hydrogen, ($M_{H_2} = 2\ g\ mol^{-1}$).

At the cathode side, the oxygen or air flow rate is consumed for the electrochemical reaction, which was calculated by Eqs. (21) or (22), respectively:

$$\dot{m}_{O_2} = \frac{N_{cell} \times I_{cell}}{4F} M_{O_2} \quad (21)$$

$$\dot{m}_{air} = \frac{N_{cell} \times I_{cell}}{4F \times 0.21} M_{air} \quad (22)$$

Where: M_{O_2} and M_{air} represent the molar mass of oxygen, ($M_{O_2} = 32\ g\ mol^{-1}$), and molar mass of air ($M_{air} = 29\ g\ mol^{-1}$), respectively.

To evaluate the cell performance and hydrogen utilization during PEMFC operation, the energy efficiency was employed and defined following the lower heat value (LHV) and higher heating value (HHV), corresponding to Eqs. (23) and (24):

Table 2
Input parameter for the model in this study

Parameter	Value	Unit	Reference
$i_{0,c}$	10^{-4}	A cm^{-2}	(Larminie *et al.*, 2003)
$i_{0,a}$	10^{-3}	A cm^{-2}	(Larminie et al., 2003)
α_a, α_c	0.5	–	(You *et al.*, 2017)
t_m	178	μm	(Xue *et al.*, 2006)
A_{cell}	25	cm²	Well know
r_i	0.0003	Ω	(Xue *et al.*, 2006)
a_m	0.5	–	(Zhu *et al.*, 2019)
T	303–353	K	Well know
P_{H_2}	1.0 – 3.5	atm	Well know
P_{O_2}	1.0 – 3.5	atm	Well know
h_m	0.01284	m s^{-1}	(Reshetenko & St-Pierre, 2014)
C_{in}	40	mol m^{-3}	Assumed
C_{out}	5	mol m^{-3}	Assumed

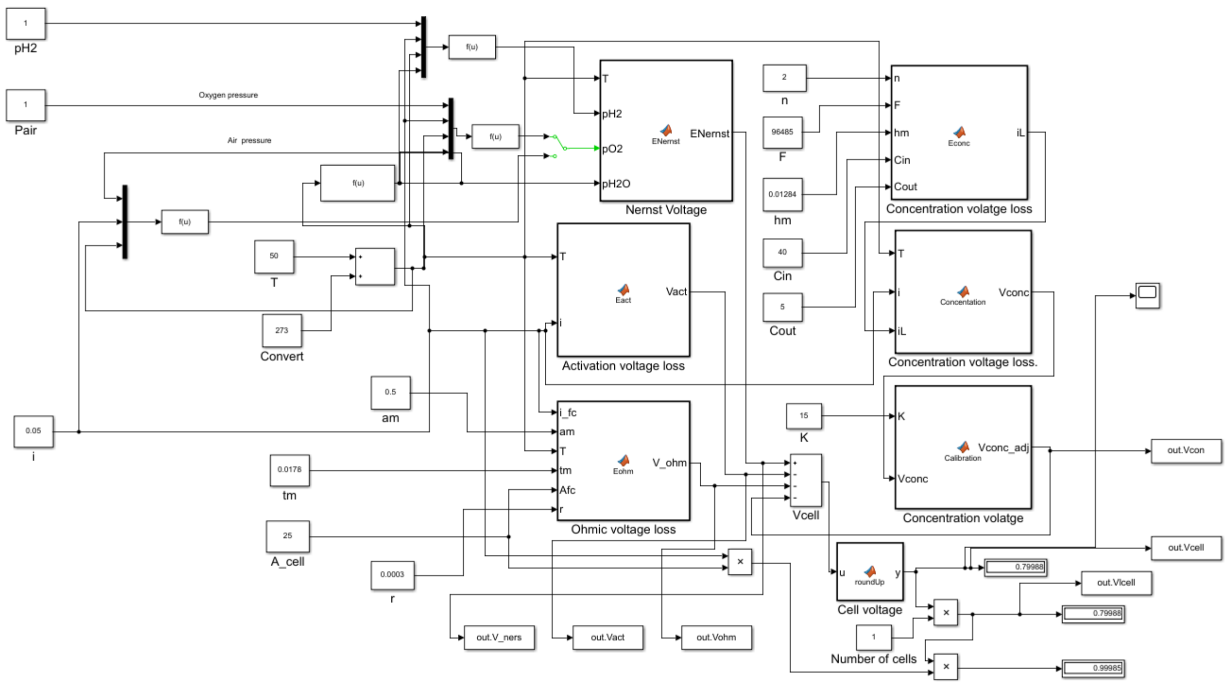

Fig. 2 Mathematical model in Matlab/Simulink for this study

$$\eta_{fc\_HHV} = \frac{V_{cell}}{1.48} \tag{23}$$

$$\eta_{fc\_LHV} = \frac{V_{cell}}{1.25} \tag{24}$$

2.2.9 Boundary conditions for the model

In this study, PEMFC performance is investigated under steady-state operating conditions. To simplify the model and facilitate its evaluation, several assumptions are made, as follows:

(1) The cell operating temperature is uniform throughout the PEMFC during operation at a given temperature.
(2) The operating pressure is identical along the flow-field channels.
(3) The operating current density is uniformly distributed across the current collectors.
(4) During fabrication of the membrane–electrode assembly (MEA), the catalyst layer is uniformly distributed over the active cell area.
(5) The reactant gases are treated as ideal gases during PEMFC operation.

To perform the simulations, the input parameters used in the model are summarized in Table 2. These parameters include all the necessary inputs required for model implementation. Additionally, the mathematical model in MATLAB/Simulink software for this study is illustrated in Fig. 2. The basic blocks from the MATLAB/Simulink library were used to develop this model, including the Transfer Function block, Constant block, Mux block, Sum block, and Display block. To obtain the model results, the Go To block was employed, and the data were extracted to the Workspace environment.

3. Results and discussion

3.1 Validation of the model in this study

To evaluate the accuracy of the proposed model, validation was performed by varying the operating temperature and current density. Under steady-state conditions, the resulting cell voltage characteristics are presented in Fig. 3(a) in the form of polarization curves. It can be observed that an increase in operating temperature leads to a higher cell voltage due to enhanced electrochemical reaction kinetics and improved electrical conductivity. The obtained polarization curves are consistent with those reported in previous studies (Dannenberg *et al.*, 2000; Diab *et al.*, 2025; Ge & Yi, 2003; Omran *et al.*, 2021; Santarelli & Torchio, 2007; Tsai *et al.*, 2006). Therefore, the model developed in this study is validated and shows good agreement with the results reported in the literature.

3.2 Effect of operating temperature on PEMFC performance

During PEMFC operation, the operating temperature has a significant impact on cell performance. In this section, to investigate the effect of operating temperature on PEMFC performance, the operating pressures at the anode and cathode are fixed at 1 atm and 1.5 atm, respectively. The cell active area is set to 25 cm^2.

Fig. 3 presents the cell voltage behavior under varying operating temperatures ranging from 30 to 80 °C. It can be observed that operating temperature has a significant influence on PEMFC performance. Fig. 3(a) illustrates the polarization curves of PEMFC performance under varying operating temperatures. It can be observed that an increase in operating temperature generally enhances cell performance due to improved electrochemical reaction kinetics, increased thermal efficiency, and higher physical exergy efficiency of hydrogen and oxygen (Atak *et al.*, 2023). At moderate temperatures, both activation and ohmic voltage losses decrease significantly with increasing operating current density and temperature, which contributes to improved cell performance. However, when the PEMFC operates at temperatures above 70 °C, a deterioration in performance is observed. This behavior can be attributed to membrane dehydration at elevated temperatures, which reduces proton conductivity and, consequently, lowers the output cell voltage (Bose *et al.*, 2011). Therefore, effective thermal management is critical for maintaining optimal PEMFC

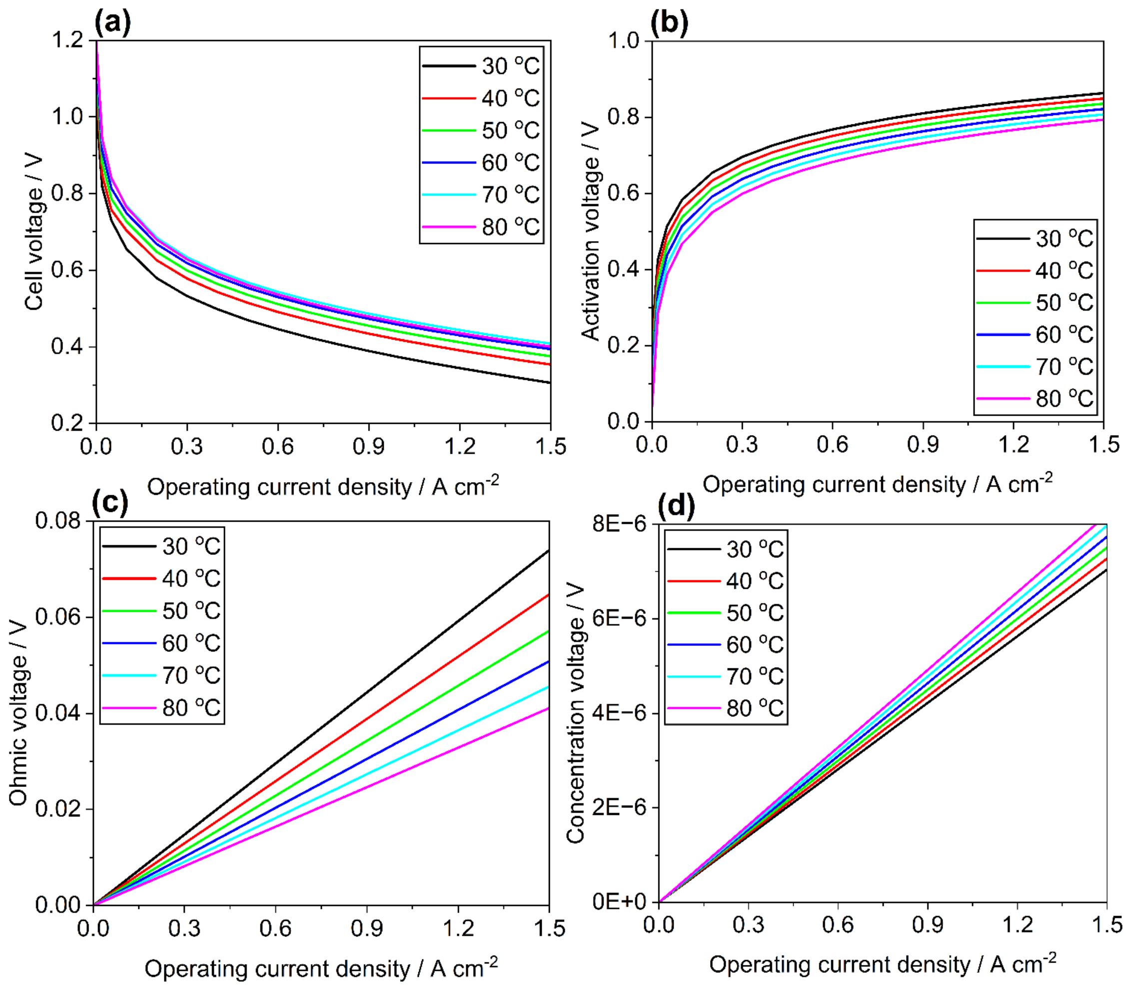

Fig. 3 Effect of operating temperature on cell voltage (a); Activation voltage (b); Ohmic voltage (c); and concentration voltage (d)

performance and preventing performance degradation at high operating temperatures.

Specifically, as the operating temperature increases, the activation voltage loss decreases, as shown in Fig. 3(b). This improvement can be attributed to enhanced electrochemical reaction kinetics and shortened activation time at higher temperatures (Park *et al.*, 2021; Qi & Kaufman, 2002, 2003), which benefit from increased membrane water uptake and improved ionic conductivity (Alberti et al., 2008; Christmann *et al.*, 2021; Silva & Rouboa, 2012). In addition, the ohmic voltage loss also decreases with increasing operating temperature, as illustrated in Fig. 3(c). This behavior is mainly due to the reduction in ohmic resistance associated with key components, such as bipolar plates and current collectors, at elevated temperatures. In other words, the electrical conductivity of these components improves at higher operating temperatures. By contrast, the concentration voltage loss shows a slight increase with operating temperature, although the effect is not significant, as depicted in Fig. 3(d). This minor increase can be explained by the reduction in gas concentration at higher temperatures, which leads to reactant gas dilution and a marginal rise in concentration-related losses.

3.3 Effect of operating pressure on PEMFC performance

Operating pressure significantly affects PEMFC performance and is therefore considered in this study. To evaluate the influence of operating pressure on PEMFC performance, the operating temperature is fixed at 60 °C. The pressures at the anode, cathode, and both electrodes are then varied to examine their respective effects on cell performance.

Fig. 4(a) presents the PEMFC polarization curves under various anode operating pressures, increased in increments of 0.5 atm. It can be observed that cell performance improves as the anode operating pressure increases. This improvement can be attributed to the increase in partial pressures of reactants and products, which enhances the Nernst potential at higher pressures (Santarelli & Torchio, 2007). In addition, a higher anode operating pressure promotes proton production from hydrogen, thereby enhancing electrochemical reaction kinetics. Moreover, increasing pressure reduces membrane resistance and interface contact resistance, leading to a decrease in voltage losses and an improvement in cell voltage. At a current density of 0.5 A cm^{-2}, the cell voltages are 0.550, 0.559, 0.564, 0.568, 0.571, and 0.574 V for anode operating pressures of 1.0, 1.5, 2.0, 2.5, 3.0, and 3.5 atm, respectively.

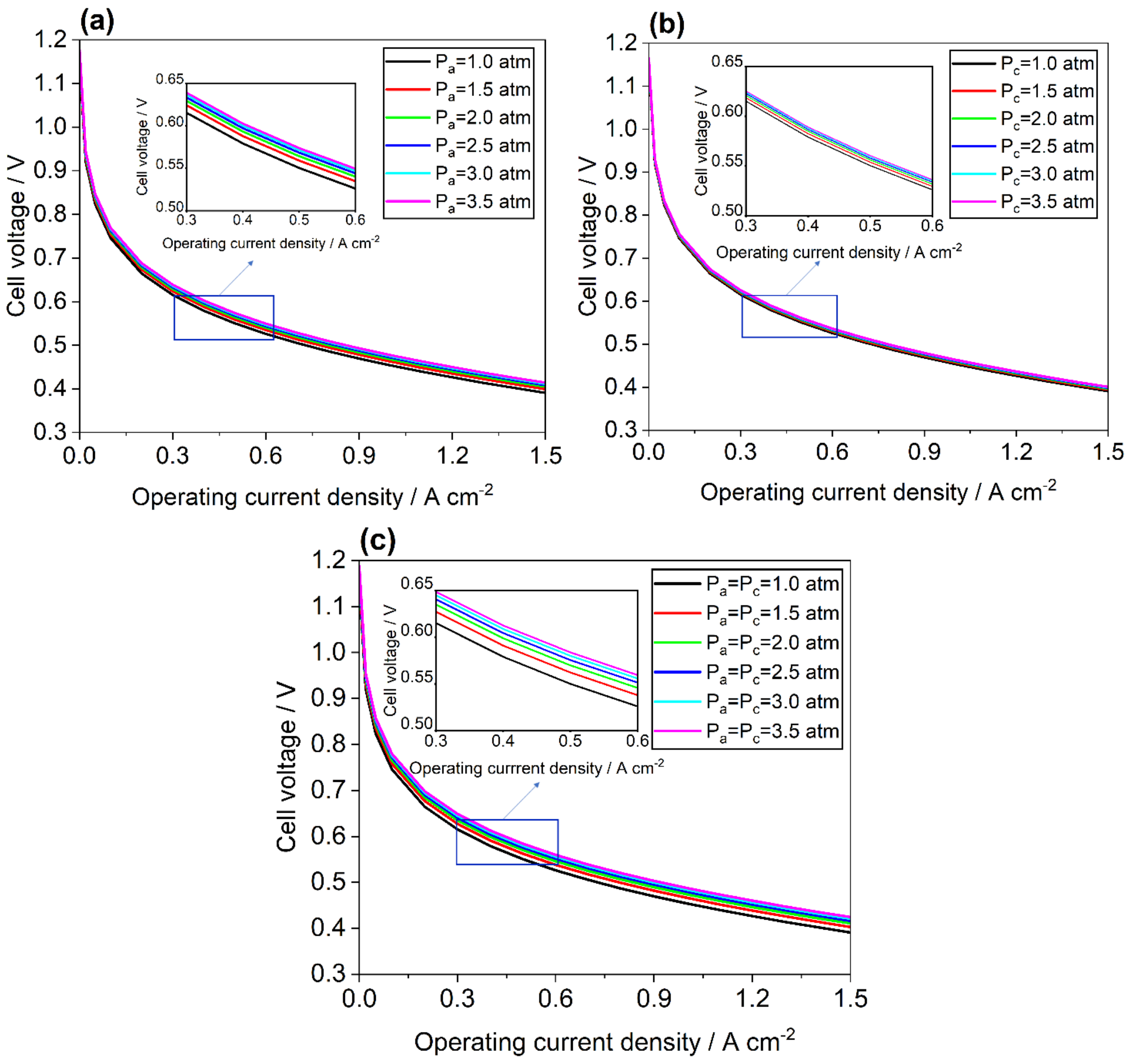

Fig. 4 Cell voltage under varying anode operating pressures (a); cathode operating pressures (b); and both anode and cathode operating pressures (c)

To evaluate the effect of cathode operating pressure on PEMFC performance, the cathode pressure is varied from 1.0 to 3.5 atm in increments of 0.5 atm. Fig. 4(b) illustrates the relationship between operating current density and cell performance under different cathode operating pressures. Similar to the anode pressure case, an increase in cathode operating pressure leads to improved cell performance due to enhanced electrochemical reaction kinetics and an increase in the Nernst voltage. However, compared with the anode pressure case, the cell voltage achieved under varying cathode operating pressures is lower. This behavior can be attributed to the sluggish kinetics of the oxygen reduction reaction (ORR) at the cathode (Stacy *et al.*, 2017).

Fig. 4(c) illustrates the relationship between operating current density and cell voltage under simultaneous variation of both anode and cathode operating pressures. It can be observed that increasing the operating pressure results in a higher cell voltage. This behavior can be explained by the same mechanisms discussed in the previous cases. The results clearly indicate that cell performance improves as the operating pressure increases.

3.4 Effect of membrane thickness on PEMFC performance

To evaluate the effect of membrane thickness on PEMFC performance, the operating temperature is fixed at 50 °C, while the anode and cathode operating pressures are set to 1 atm and 1.5 atm, respectively. Fig. 5 illustrates the influence of membrane thickness on cell performance and ohmic voltage loss. It can be observed that increasing membrane thickness leads to a decrease in cell voltage, as shown in Fig. 5(a). This behavior is primarily caused by an increase in ohmic voltage loss. As the membrane thickness increases, proton transport from the anode to the cathode becomes more difficult, resulting in higher ionic resistance and a reduction in the PEMFC output voltage, as depicted in Fig. 5(b). To further clarify the effect of membrane thickness on cell voltage and ohmic resistance, the corresponding values for different membrane thicknesses are summarized in Table 3. The results indicate that ohmic voltage loss increases with increasing membrane thickness. Among the membranes considered, Nafion 117 has the greatest thickness and therefore exhibits the highest ohmic voltage loss of 0.046 V, resulting in a reduced cell voltage of 0.412 V.

3.5 Effect of cathode gas type on PEMFC performance

Under an operating temperature of 50 °C, with anode and cathode pressures of 1.0 atm and 1.5 atm, respectively, and a cell active area of 25 cm^2, the effect of different cathode supply gases on PEMFC performance is investigated. Hydrogen is supplied to the anode, while either pure oxygen or air is supplied to the cathode.

Fig. 6(a) compares the PEMFC performance when using pure oxygen and air at the cathode. It can be observed that the cell performance with pure oxygen is higher than that with air. This improvement is attributed to the higher oxygen concentration, which enhances the electrochemical reaction kinetics at the cathode. In contrast, when air is supplied to the cathode, the lower oxygen concentration leads to slower oxygen reduction reaction kinetics, thereby reducing cell performance (Stacy *et al.*, 2017).

3.6 Effect of the number of cells in a stack on PEMFC performance

In practical applications, single PEMFCs are connected in series to achieve a higher output voltage, forming what is known as a PEMFC stack. Therefore, the effect of the number of cells in a stack on PEMFC performance is evaluated in this study. The operating temperature is fixed at 60 °C, while the anode and cathode pressures are set to 1.0 atm and 1.5 atm, respectively. A cell active area of 25 cm^2 is employed, and air is supplied to the cathode.

Table 3
Ohmic voltage loss and cell voltage under varying membrane types at a load level of 1.2 A cm^{-2}

Nafion code	Thickness / cm	η_{ohmic} / V	V_{cell} /V
Gore-Select	0.003	0.008	0.449
112	0.0051	0.013	0.444
1135	0.0091	0.024	0.434
115	0.0127	0.033	0.425
117	0.0178	0.046	0.412

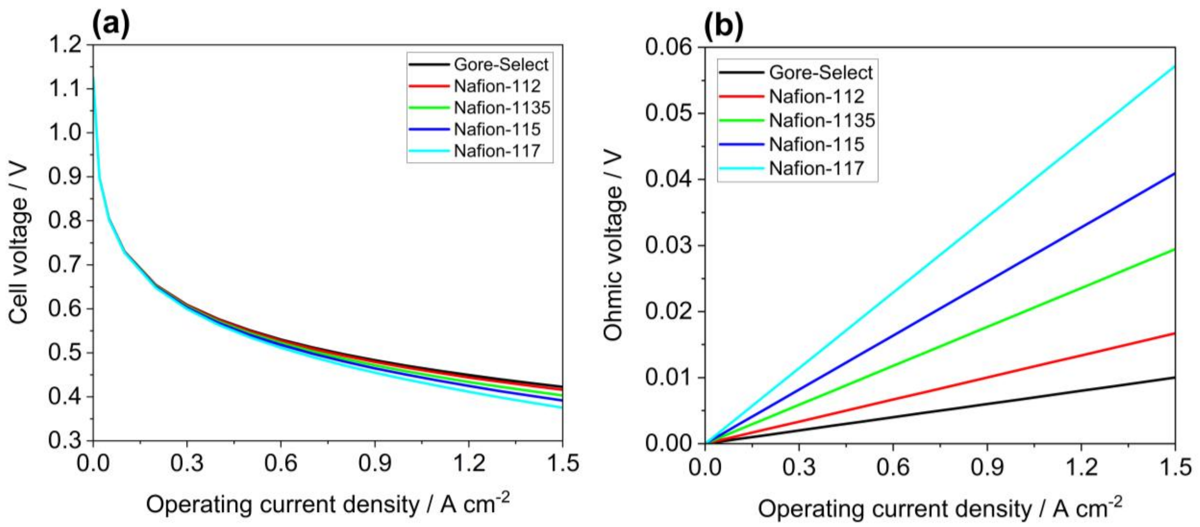

Fig. 5 Effect of membrane thickness on cell voltage (a) and ohmic voltage (b)

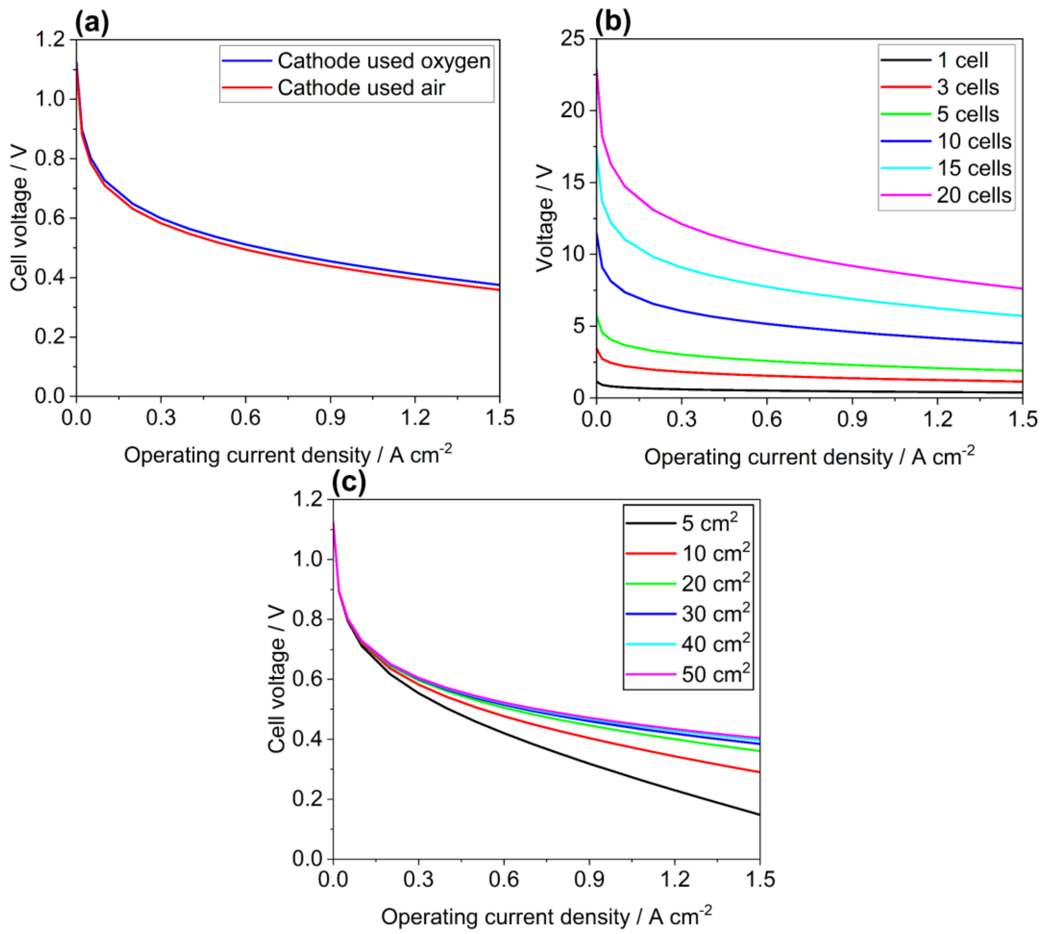

Fig. 6 PEMFC performance under different supplied oxygen or air at the cathode sides (a); Number of cells (b); and cell activation area (c)

The number of cells in the stack is varied as 1, 3, 5, 10, 15, and 20. Fig. 6(b) illustrates the relationship between the number of cells and the PEMFC output voltage. It can be observed that the output voltage increases with the number of cells connected in series. Specifically, as the number of cells increases, the voltage slope becomes steeper due to the cumulative effect of overpotentials across the stack.

3.7 Effect of cell activation area on PEMFC performance

The cell active area has a significant effect on PEMFC performance. Fig. 6(c) illustrates the cell voltage under various active areas of 5, 10, 20, 30, 40, and 50 cm^2. It can be observed that increasing the cell active area leads to an improvement in cell voltage. This improvement can be attributed to the larger reaction area available for electrochemical processes, which facilitates more effective utilization of the reactant gases. Consequently, for a given operating current density, increasing the cell active area enhances the output voltage of the PEMFC.

3.8 Effect of load level on water management and heat generation in PEMFC

In this section, water and heat generation resulting from the electrochemical reactions in the PEMFC are analyzed. To evaluate water and heat generation, the operating conditions are set with a cell active area of 25 cm^2, a stack consisting of 20 cells, and an operating temperature of 50 °C. During PEMFC operation under load, water and heat are generated as a result of electrochemical reactions. Fig. 7 illustrates the relationship between load level and water generation. It can be observed that water production increases with increasing load level, which can be attributed to intensified electrochemical reactions at higher currents. In general, moderate heat and water generation can enhance PEMFC performance by maintaining adequate membrane hydration and promoting electrochemical reaction kinetics. However, excessive operating temperature may lead to membrane dehydration, resulting in reduced proton conductivity and a decline in output voltage. Conversely, at high operating current densities, excessive water generation may cause flooding within the PEMFC, obstructing reactant transport and reducing cell voltage. Therefore, effective water and thermal management are critical for achieving optimal PEMFC performance.

3.9 Discussion on the gas consumption and energy efficiency

In this study, the consumption of hydrogen, oxygen, and air during PEMFC operation is analyzed, and the corresponding energy efficiency is also evaluated. In this section, the anode and cathode operating pressures are fixed at 1.0 atm and 1.5 atm, respectively. Fig. 8(a) illustrates the gas consumption of the PEMFC under different load levels. As the load increases, gas consumption rises accordingly to sustain the electrochemical reactions. When the load current increases from 0 to 25 A, hydrogen consumption increases from 0 to 0.0052 g s^{-1}, oxygen consumption ranges from 0 to 0.0415 g s^{-1}, and air consumption ranges from 0 to 0.1789 g s^{-1}.

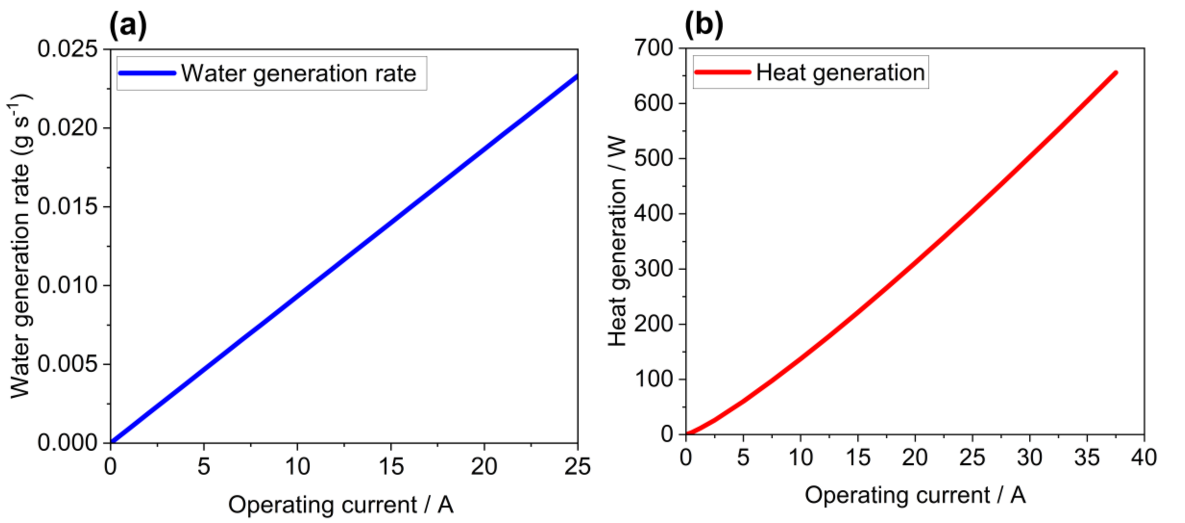

Fig. 7 Product generation from the electrochemical reaction (a) Water generation; (b) Heat generation

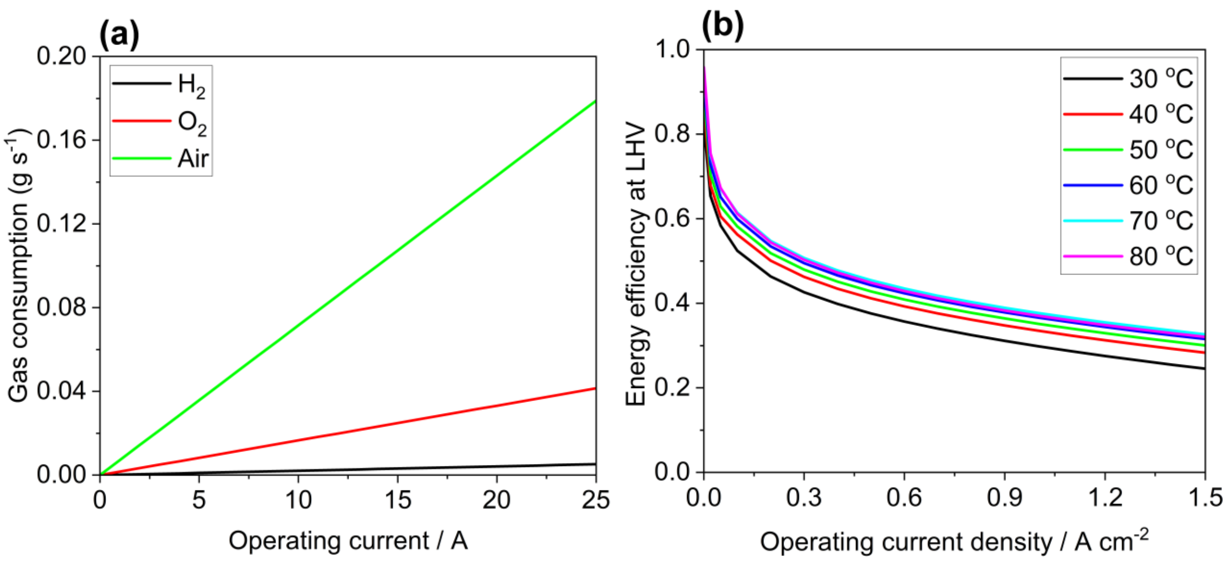

Fig. 8 (a) Gas consumption and (b) Energy efficiency of the PEMFC

Fig. 8(b) illustrates the energy efficiency of the PEMFC under varying current densities and operating temperatures. It can be observed that energy efficiency decreases with increasing current density, primarily due to enhanced voltage losses. In particular, when the operating temperature exceeds 70 °C, a noticeable decline in energy efficiency occurs. This behavior can be attributed to membrane dehydration at elevated temperatures, which increases overpotential, reduces cell voltage, and consequently decreases overall energy efficiency.

4. Conclusion

In this study, a mathematical model was developed using the MATLAB/Simulink environment to investigate the effects of operating conditions on PEMFC performance under steady-state conditions. Several conclusions can be drawn in this study. Indeed, a high-precision mathematical model was successfully developed to analyze and discuss PEMFC performance. The key operating temperature and pressure were found to have a significant impact on PEMFC performance. On the other hand, water and heat generation resulting from electrochemical reactions play a critical role in influencing PEMFC performance in this study. Aditionally, the gas utilization and energy efficiency were analyzed in detail to provide further insight into PEMFC operation.

In summary, the developed model provides a reliable tool for accurately predicting PEMFC performance under various steady-state operating conditions.

Acknowledgments

The author would like to express thanks to Lac Hong University for their financial support in completing this study.

Author Contributions: T.T.D: Conceptualization, methodology, formal analysis, writing—original draft, project administration, writing—review and editing, validation, supervision T.K.V.; writing—original draft, resources, methodology, C.S.P.; writing—original draft, methodology, validation. All authors have read and agreed to the published version of the manuscript.

Funding: This research was funded by Lac Hong University for the research and publication of this article.

Conflicts of Interest: The authors declare no conflict of interest.

References

Alberti, G., Narducci, R., & Sganappa, M. (2008). Effects of hydrothermal/thermal treatments on the water-uptake of Nafion membranes and relations with changes of conformation, counter-elastic force and tensile modulus of the matrix. *Journal of power sources*, *178*(2), 575-583. https://doi.org/10.1016/j.jpowsour.2007.09.034

Amirfazli, A., Asghari, S., & Sarraf, M. (2018). An investigation into the effect of manifold geometry on uniformity of temperature distribution in a PEMFC stack. *Energy*, *145*, 141-151. https://doi.org/10.1016/j.energy.2017.12.124

Arat, H. T., & Çeper, B. A. (2025). Investigation of instantaneous temperature variations in hydrogen PEM fuel cell stack under cold climate conditions. *International Journal of Hydrogen Energy*, *107*, 539-547. https://doi.org/10.1016/j.ijhydene.2024.07.294

Atak, N. N., Dogan, B., & Yesilyurt, M. K. (2023). Investigation of the performance parameters for a PEMFC by thermodynamic analyses: Effects of operating temperature and pressure. *Energy*, *282*, 128907. https://doi.org/10.1016/j.energy.2023.128907

Barbir, F. (2012). *PEM fuel cells: theory and practice*. Academic press.

Bates, A., Mukherjee, S., Hwang, S., Lee, S. C., Kwon, O., Choi, G. H., & Park, S. (2013). Simulation and experimental analysis of the clamping pressure distribution in a PEM fuel cell stack. *International Journal of Hydrogen Energy*, *38*(15), 6481-6493. https://doi.org/10.1016/j.ijhydene.2013.03.049

Belkhiri, Z., Zeroual, M., Moussa, H. B., & Zitouni, B. (2011). Effect of temperature and water content on the performance of PEM fuel cell. *Journal of Renewable Energies*, *14*(1), 121-130. https://doi.org/10.54966/jreen.v14i1.246

Boas, J. V., Oliveira, V. B., Simões, M., & Pinto, A. M. (2022). Review on microbial fuel cells applications, developments and costs. *Journal of Environmental Management*, *307*, 114525. https://doi.org/10.1016/j.jenvman.2022.114525

Bose, S., Kuila, T., Nguyen, T. X. H., Kim, N. H., Lau, K.-t., & Lee, J. H. (2011). Polymer membranes for high temperature proton exchange membrane fuel cell: Recent advances and challenges. *Progress in Polymer Science*, *36*(6), 813-843. https://doi.org/10.1016/j.progpolymsci.2011.01.003

Carrette, L., Friedrich, K., & Stimming, U. (2001). Fuel cells-fundamentals and applications. *Fuel Cells*, *1*.

Chang, W., Hwang, J., Weng, F., & Chan, S. (2007). Effect of clamping pressure on the performance of a PEM fuel cell. *Journal of power sources*, *166*(1), 149-154. https://doi.org/10.1016/j.jpowsour.2007.01.015

Chen, J.-H., He, P., Cai, S.-J., He, Z.-H., Zhu, H.-N., Yu, Z.-Y., Yang, L.-Z., & Tao, W.-Q. (2024). Modeling and temperature control of a water-cooled PEMFC system using intelligent algorithms. *Applied energy*, *372*, 123790. https://doi.org/10.1016/j.apenergy.2024.123790

Chen, T., Liu, S., Zhang, J., & Tang, M. (2019). Study on the characteristics of GDL with different PTFE content and its effect on the performance of PEMFC. *International Journal of Heat and Mass Transfer*, *128*, 1168-1174. https://doi.org/10.1016/j.ijheatmasstransfer.2018.09.097

Christmann, K., Friedrich, K. A., & Zamel, N. (2021). Activation mechanisms in the catalyst coated membrane of PEM fuel cells. *Progress in Energy and Combustion Science*, *85*, 100924. https://doi.org/10.1016/j.pecs.2021.100924

Chugh, S., Chaudhari, C., Sonkar, K., Sharma, A., Kapur, G., & Ramakumar, S. (2020). Experimental and modelling studies of low temperature PEMFC performance. *International Journal of Hydrogen Energy*, *45*(15), 8866-8874. https://doi.org/10.1016/j.ijhydene.2020.01.019

Dannenberg, K., Ekdunge, P., & Lindbergh, G. (2000). Mathematical model of the PEMFC. *Journal of Applied Electrochemistry*, *30*(12), 1377-1387. https://doi.org/10.1023/A:1026534931174

Diab, A. A. Z., Ali, A. H., Sultan, H. M., Ismeil, M. A., & Abdelsattar, M. (2025). Novel mathematical modeling parameters of PEMFC based on Newton-Raphson iterative method. *IEEE Access*. https://doi.org/10.1109/ACCESS.2025.3580704

Ding, F., Zou, T., Wei, T., Chen, L., Qin, X., Shao, Z., & Yang, J. (2023). The pinhole effect on proton exchange membrane fuel cell (PEMFC) current density distribution and temperature distribution. *Applied energy*, *342*, 121136. https://doi.org/10.1016/j.apenergy.2023.121136

Dyer, C. K. (2002). Fuel cells for portable applications. *Journal of power sources*, *106*(1-2), 31-34. https://doi.org/10.1016/S0378-7753(01)01069-2

Faddeev, N., Anisimov, E., Belichenko, M., Kuriganova, A., & Smirnova, N. (2021). Investigation of the ambient temperature influence on the PEMFC characteristics: Modeling from a single cell to a stack. *Processes*, *9*(12), 2117. https://doi.org/10.3390/pr9122117

Flick, S., Schwager, M., McCarthy, E., & Mérida, W. (2014). Designed experiments to characterize PEMFC material properties and performance. *Applied energy*, *129*, 135-146. https://doi.org/10.1016/j.apenergy.2014.05.009

Ge, S.-H., & Yi, B.-L. (2003). A mathematical model for PEMFC in different flow modes. *Journal of power sources*, *124*(1), 1-11. https://doi.org/10.1016/S0378-7753(03)00584-6

Ghasemi, M., Ramiar, A., Ranjbar, A., & Rahgoshay, S. (2017). A numerical study on thermal analysis and cooling flow fields effect on PEMFC performance. *International Journal of Hydrogen Energy*, *42*(38), 24319-24337. https://doi.org/10.1016/j.ijhydene.2017.08.036

Giner-Sanz, J. J., Ortega, E., & Pérez-Herranz, V. (2015). Statistical analysis of the effect of the temperature and inlet humidities on the parameters of a PEMFC model. *Fuel Cells*, *15*(3), 479-493. https://doi.org/10.1002/fuce.201400163

González, G. C., Toharias, B., Rosa, F., Guerra, J., & Iranzo, A. (2025). Temperature and Current Density distributions in a 100 cm2 PEM Fuel Cell: Effects of flow field designs. *Journal of power sources*, *652*, 237625. https://doi.org/10.1016/j.jpowsour.2025.237625

Hao, H., Mo, R., Kang, S., & Wu, Z. (2023). Effects of temperature, inlet gas pressure and humidity on PEM water contents and current density distribution. *Results in Engineering*, *20*, 101411. https://doi.org/10.1016/j.rineng.2023.101411

Hu, D., Wang, Y., Li, J., Yang, Q., & Wang, J. (2021). Investigation of optimal operating temperature for the PEMFC and its tracking control for energy saving in vehicle applications. *Energy Conversion and Management*, *249*, 114842. https://doi.org/10.1016/j.enconman.2021.114842

Jomori, S., Nonoyama, N., & Yoshida, T. (2012). Analysis and modeling of PEMFC degradation: Effect on oxygen transport. *Journal of power sources*, *215*, 18-27. https://doi.org/10.1016/j.jpowsour.2012.04.069

Kim, S., & Hong, I. (2008). Effects of humidity and temperature on a proton exchange membrane fuel cell (PEMFC) stack. *Journal of Industrial and Engineering Chemistry*, *14*(3), 357-364. https://doi.org/10.1016/j.jiec.2008.01.007

Larbi, B., Alimi, W., Chouikh, R., & Guizani, A. (2013). Effect of porosity and pressure on the PEM fuel cell performance. *International Journal of Hydrogen Energy*, *38*(20), 8542-8549. https://doi.org/10.1016/j.ijhydene.2012.11.022

Laribi, S., Mammar, K., Sahli, Y., & Koussa, K. (2018). Air supply temperature impact on the PEMFC impedance. *Journal of Energy Storage*, *17*, 327-335. https://doi.org/10.1016/j.est.2018.03.020

Larminie, J., Dicks, A., & McDonald, M. S. (2003). *Fuel cell systems explained* (Vol. 2). J. Wiley Chichester, UK.
Lee, C.-I., & Chu, H.-S. (2007). Effects of temperature on the location of the gas–liquid interface in a PEM fuel cell. *Journal of power sources*, *171*(2), 718-727. https://doi.org/10.1016/j.jpowsour.2007.06.019
Lee, H., Jeong, S., Song, J., Kim, M., Chu, C., Lee, Y., Kim, D., & Kim, M. (2023). Influence of PEMFC degradation on its performance in different temperature and relative humidity conditions. *Journal of Mechanical Science and Technology*, *37*(4), 2095-2108. https://doi.org/10.1007/s12206-023-0345-5
Li, B., Wu, Z., Li, Y., He, J., Wang, B., Jiao, K., Hu, X., Fan, H., & Wu, J. (2025). Thermal-water-electrical coupling modeling of PEMFC and its dynamic performance analysis under different operating conditions. *Applied energy*, *398*, 126447. https://doi.org/10.1016/j.apenergy.2025.126447
Lu, J., Wei, G., Zhu, F., Yan, X., & Zhang, J. (2019). Pressure effect on the PEMFC performance. *Fuel Cells*, *19*(3), 211-220. https://doi.org/10.1002/fuce.201800135
Mohtadi, R., Lee, W.-K., & Van Zee, J. (2005). The effect of temperature on the adsorption rate of hydrogen sulfide on Pt anodes in a PEMFC. *Applied Catalysis B: Environmental*, *56*(1-2), 37-42. https://doi.org/10.1016/j.apcatb.2004.08.012
Murthy, M., Esayian, M., Lee, W.-k., & Van Zee, J. (2002). The effect of temperature and pressure on the performance of a PEMFC exposed to transient CO concentrations. *Journal of the Electrochemical Society*, *150*(1), A29. https://doi.org/10.1149/1.1522383
Mus, J., Nuyttens, R., Vanierschot, M., Vandeginste, V., & Buysschaert, F. (2025). Experimental study of the effects of ambient conditions on the performance of open-cathode PEM fuel cells. *Journal of power sources*, *660*, 238467. https://doi.org/10.1016/j.jpowsour.2025.238467
Neyerlin, K., Gasteiger, H. A., Mittelsteadt, C. K., Jorne, J., & Gu, W. (2005). Effect of relative humidity on oxygen reduction kinetics in a PEMFC. *Journal of the Electrochemical Society*, *152*(6), A1073. https://doi.org/10.1149/1.1897368
Noorkami, M., Robinson, J. B., Meyer, Q., Obeisun, O. A., Fraga, E. S., Reisch, T., Shearing, P. R., & Brett, D. J. (2014). Effect of temperature uncertainty on polymer electrolyte fuel cell performance. *International Journal of Hydrogen Energy*, *39*(3), 1439-1448. https://doi.org/10.1016/j.ijhydene.2013.10.156
Omran, A., Lucchesi, A., Smith, D., Alaswad, A., Amiri, A., Wilberforce, T., Sodré, J. R., & Olabi, A. (2021). Mathematical model of a proton-exchange membrane (PEM) fuel cell. *International Journal of Thermofluids*, *11*, 100110. https://doi.org/10.1016/j.ijft.2021.100110
Ou, K., Yuan, W.-W., Choi, M., Yang, S., & Kim, Y.-B. (2017). Performance increase for an open-cathode PEM fuel cell with humidity and temperature control. *International Journal of Hydrogen Energy*, *42*(50), 29852-29862. https://doi.org/10.1016/j.ijhydene.2017.10.087
Ozen, D. N., Timurkutluk, B., & Altinisik, K. (2016). Effects of operation temperature and reactant gas humidity levels on performance of PEM fuel cells. *Renewable and Sustainable Energy Reviews*, *59*, 1298-1306. https://doi.org/10.1016/j.rser.2016.01.040
Park, J., & Li, X. (2006). Effect of flow and temperature distribution on the performance of a PEM fuel cell stack. *Journal of power sources*, *162*(1), 444-459. https://doi.org/10.1016/j.jpowsour.2006.07.030
Park, J. Y., Lim, I. S., Choi, E. J., Lee, Y. H., & Kim, M. S. (2021). Comparative study of reverse flow activation and conventional activation with polymer electrolyte membrane fuel cell. *Renewable Energy*, *167*, 162-171. https://doi.org/10.1016/j.renene.2020.11.069
Qi, Z., & Kaufman, A. (2002). Activation of low temperature PEM fuel cells. *Journal of power sources*, *111*(1), 181-184. https://doi.org/10.1016/S0378-7753(02)00273-2
Qi, Z., & Kaufman, A. (2003). Quick and effective activation of proton-exchange membrane fuel cells. *Journal of power sources*, *114*(1), 21-31. https://doi.org/10.1016/S0378-7753(02)00587-6
Radhakrishnan, V., & Haridoss, P. (2011). Effect of GDL compression on pressure drop and pressure distribution in PEMFC flow field. *International Journal of Hydrogen Energy*, *36*(22), 14823-14828. https://doi.org/10.1016/j.ijhydene.2011.05.185
Reshetenko, T. V., & St-Pierre, J. (2014). Separation method for oxygen mass transport coefficient in gas and ionomer phases in PEMFC GDE. *Journal of the Electrochemical Society*, *161*(10), F1089. https://doi.org/10.1149/2.1021410jes
Rohendi, D., Majlan, E., Mohamad, A., Daud, W., Kadhum, A., & Shyuan, L. (2015). Effects of temperature and backpressure on the performance degradation of MEA in PEMFC. *International Journal of Hydrogen Energy*, *40*(34), 10960-10968. https://doi.org/10.1016/j.ijhydene.2015.06.161
Santarelli, M., & Torchio, M. F. (2007). Experimental analysis of the effects of the operating variables on the performance of a single PEMFC. *Energy Conversion and Management*, *48*(1), 40-51. https://doi.org/10.1016/j.enconman.2006.05.013
Santarelli, M. G., Torchio, M. F., & Cochis, P. (2006). Parameters estimation of a PEM fuel cell polarization curve and analysis of their behavior with temperature. *Journal of power sources*, *159*(2), 824-835. https://doi.org/10.1016/j.jpowsour.2005.11.099
Shan, Y., & Choe, S.-Y. (2006). Modeling and simulation of a PEM fuel cell stack considering temperature effects. *Journal of power sources*, *158*(1), 274-286. https://doi.org/10.1016/j.jpowsour.2005.09.053
Silva, V. B., & Rouboa, A. (2012). An activation procedure applied to fluorinated and non-fluorinated proton exchange membranes. *Fuel processing technology*, *103*, 27-33. https://doi.org/10.1016/j.fuproc.2011.12.042
Stacy, J., Regmi, Y. N., Leonard, B., & Fan, M. (2017). The recent progress and future of oxygen reduction reaction catalysis: A review. *Renewable and Sustainable Energy Reviews*, *69*, 401-414. https://doi.org/10.1016/j.rser.2016.09.135
Tang, X., Zhang, Y., & Xu, S. (2023). Temperature sensitivity characteristics of PEM fuel cell and output performance improvement based on optimal active temperature control. *International Journal of Heat and Mass Transfer*, *206*, 123966. https://doi.org/10.1016/j.ijheatmasstransfer.2023.123966
Tiss, F., Chouikh, R., & Guizani, A. (2013). Dynamic modeling of a PEM fuel cell with temperature effects. *International Journal of Hydrogen Energy*, *38*(20), 8532-8541. https://doi.org/10.1016/j.ijhydene.2012.09.101
Tsai, C., Chen, F., Ruo, A., Chang, M.-H., Chu, H.-S., Soong, C., Yan, W., & Cheng, C. (2006). An analytical solution for transport of oxygen in cathode gas diffusion layer of PEMFC. *Journal of power sources*, *160*(1), 50-56. https://doi.org/10.1016/j.jpowsour.2006.01.019
Waller, M. G., Walluk, M. R., & Trabold, T. A. (2016). Performance of high temperature PEM fuel cell materials. Part 1: Effects of temperature, pressure and anode dilution. *International Journal of Hydrogen Energy*, *41*(4), 2944-2954. https://doi.org/10.1016/j.ijhydene.2015.12.069
Wang, Y., Sun, Z., & Yang, L. (2025). Optimizing temperature distribution in a PEMFC stack: A computational study on cooling plate and coolant dynamics. *International Journal of Hydrogen Energy*, *97*, 88-103. https://doi.org/10.1016/j.ijhydene.2024.11.339
Xia, L., Ni, M., He, Q., Xu, Q., & Cheng, C. (2021). Optimization of gas diffusion layer in high temperature PEMFC with the focuses on thickness and porosity. *Applied energy*, *300*, 117357. https://doi.org/10.1016/j.apenergy.2021.117357
Xue, X., Cheng, K. W. E., & Sutanto, D. (2006). Unified mathematical modelling of steady-state and dynamic voltage–current characteristics for PEM fuel cells. *Electrochimica acta*, *52*(3), 1135-1144. https://doi.org/10.1016/j.electacta.2006.07.011
You, X., Ye, Q., & Cheng, P. (2017). The dependence of mass transfer coefficient on the electrolyte velocity in carbon felt electrodes: determination and validation. *Journal of the Electrochemical Society*, *164*(11), E3386. https://doi.org/10.1149/2.0401711jes
Zhao, D., Gao, F., Massonnat, P., Dou, M., & Miraoui, A. (2015). Parameter sensitivity analysis and local temperature distribution effect for a PEMFC system. *IEEE transactions on energy conversion*, *30*(3), 1008-1018. https://doi.org/10.1109/TEC.2015.2404793
Zhao, J., Cheng, X., Zhong, Z., Ma, Y., & Zhou, C. (2025). Experimental investigation on temperature distribution and evolution of air-cooled PEMFCs under various operating conditions. *Thermal*

Science and Engineering Progress, *62*, 103665. https://doi.org/10.1016/j.tsep.2025.103665
Zhou, P., & Wu, C. (2007). Numerical study on the compression effect of gas diffusion layer on PEMFC performance. *Journal of power sources*, *170*(1), 93-100. https://doi.org/10.1016/j.jpowsour.2007.03.073
Zhu, M., Xie, X., Wu, K., Najmi, A.-U.-H., & Jiao, K. (2019). Experimental investigation of the effect of membrane water content on PEM fuel cell cold start. *Energy Procedia*, *158*, 1724-1729. https://doi.org/10.1016/j.egypro.2019.01.401